International Journal of Rock Mechanics & Mining Sciences 48 (2011) 712–727

Contents lists available at ScienceDirect

International Journal of Rock Mechanics & Mining Sciences

journal homepage: www.elsevier.com/locate/ijrmms

The distinct element analysis for hydraulic fracturing in hard rock considering fluid viscosity and particle size distribution

Hiroyuki Shimizu [a,*], Sumihiko Murata [b], Tsuyoshi Ishida [b]

[a] Department of Civil and Earth Resources Engineering, Kyoto University, Katsura, Nishikyo-ku, Kyoto 615-8540, Japan
[b] Department of Civil and Earth Resources Engineering, Kyoto University, Japan

ARTICLE INFO

Article history:
Received 15 March 2010
Received in revised form
24 November 2010
Accepted 13 April 2011
Available online 10 May 2011

Keywords:
Distinct element method (DEM)
Hydraulic fracturing
Rock
Acoustic emission (AE)
Viscosity
Particle size distribution

ABSTRACT

A series of simulations for hydraulic fracturing in competent rock was performed by using the flow-coupled DEM code to discuss the influence of the fluid viscosity and the particle size distribution. The simulation results show good agreement with experimental results that contain the AE measurement data. The following observations can be made. When a low viscosity fluid is used, the fluid infiltrates into the fracture immediately. On the other hand, when a high viscosity fluid is used, the fluid infiltrates slowly into the crack after the fracture first elongates. Although tensile cracks are dominantly generated in the simulation, the energy released from a tensile crack becomes small because the tensile strength of rock is obviously small compared with the compressive strength. Such a small AE is easily buried in a noise and difficult to be measured in an experiment. Therefore, in AE measurement experiment, shear type AE with large energy is dominantly observed, as many previous researches have indicated.

1. Introduction

To better understand the mechanics of hydraulic fracturing, a considerable amount of research has been carried out in the past few decades. According to the conventional theory, hydraulic fracturing is formed by tensile crack generation [1]. On the other hand, the shear type mechanisms was observed in most of the acoustic emission (AE) events recorded during the laboratory and field hydraulic fracturing experiments [2–5]. Ishida et al. [6] carried out a laboratory hydraulic fracturing experiments using low viscosity water and higher viscosity oil. The source mechanisms of AE events indicates that shear type mechanisms are dominant when low viscosity fluid is injected, and both shear and tensile type mechanisms are observed when high viscosity fluid is injected.

In addition, Matsunaga et al. [7] conducted hydraulic fracturing experiments for various rocks and acrylic resin, and found that rock texture, such as grain size, affects the hydraulic fracturing mechanism. Ishida et al. [6] extended this work and the hydraulic fracturing experiments were conducted for four different types of granitic rock specimens with different grain size in order to investigate the influence of grain size on induced crack geometry and fracturing mechanism [8–10]. The fault plane solutions of AE indicated that the dominant micro-fracturing mechanism becomes tensile rather than shear with decreasing grain size. Their experimental results indicate that texture of rock like grain size of granitic rocks considerably affects the geometry, surface roughness and microcracking mechanism of hydraulically induced cracks.

To give a rational explanation for such disagreement between conventional theory and AE monitoring, and to better understand the hydraulic fracturing mechanism, various numerical analysis techniques have been developed. The Finite Element Method (FEM) and the Boundary Element Method (BEM) have been commonly used to simulate hydraulic fracturing in complex three-dimensional structures [11,12]. Al-Busaidi et al. [13] simulated hydraulic fracturing in granite by using the distinct element method (DEM), and the results were compared with the AE data from the experiment. However, the simulation results showed that the disagreement mentioned above was not solved successfully. Therefore, the mechanism of hydraulic fracture propagation has not been sufficiently clarified.

In this paper, a fluid flow algorithm that can consider the fluid viscosity and permeability is introduced into the DEM program to reproduce the hydraulic fracturing. A series of simulations for hydraulic fracturing in hard rock was performed by using the flow-coupled DEM code to discuss the influence of the fluid viscosity and the particle size distribution, and to obtain insights that gave the rational explanation to the disagreement between conventional theory and the AE monitoring results.

2. Simulation methodology

2.1. Formulation of mechanics of bonded particles

The DEM for granular materials was originally developed by Cundall and Strack [14]. They developed a well-known commercially

* Corresponding author. Present address: Large-Scale Environmental Fluid Dynamics Laboratory, Institute of Fluid Science, Tohoku University, 2-1-1 Katahira Aoba-ku Sendai, 980-8577, Japan. Tel./fax: +81 22 217 5235.
E-mail address: shimizu82@gmail.com (H. Shimizu).

1365-1609/$ - see front matter © 2011 Elsevier Ltd. All rights reserved.
doi:10.1016/j.ijrmms.2011.04.013

available DEM code (particle flow code (PFC)) [15]. In this study, two-dimensional distinct element method (2D DEM) was employed, and we have written our own DEM code to study hydraulic fracturing. Since thorough details of fundamental DEM algorithm can be found in [14,15], only a summary of the primary differences between the DEM code used in this research and the parallel-bond model in the PFC^{2D} code [15] will be given.

Although the DEM is one of the numerical techniques based on the discontinuum model, it can be applied also to the continuum by introducing bonds between particles. In two dimensional DEM, the intact rock is modeled as a dense packing of small rigid circular particles. Neighboring particles are bonded together at their contact points with normal, shear, and rotational springs and interact with each other.

The increments of normal force f_n, the tangential force f_s, and the moment f_θ can be calculated from the relative motion of the bonded particles, and are given as

$$f_n = k_n(dn_j - dn_i) \tag{1}$$

$$f_s = k_s\left[ds_j - ds_i - \frac{L}{2}(d\theta_j + d\theta_i)\right] \tag{2}$$

$$f_\theta = k_\theta(d\theta_j - d\theta_i) \tag{3}$$

where k_n, k_s, and k_θ are the stiffnesses of normal, shear, and rotational springs, respectively; dn, ds, and $d\theta$ are normal and shear displacements and rotation of particles; r_i and r_j are the radii of the bonded particles. A bond between the particles is presented schematically as a gray rectangle in Fig. 1, where L and D are the bond length and the bond diameter, respectively. D is obtained from harmonic mean of the radius of two particles. L and D are given by

$$L = r_i + r_j \tag{4}$$

$$D = \frac{4r_i r_j}{r_i + r_j} \tag{5}$$

Since the DEM is formulated as a fully dynamic system, small amounts of viscous damping are necessary to provide dissipation of high-frequency vibration. If contact damping is not introduced, the assemblies will not be able to reach equilibrium. Contact damping operates on the relative velocities at the contacts and is represented by dashpots acting in the normal and shear directions at the contact points.

Since the simulation of laboratory rock tests, such as uniaxial compression test, require quasi-static loading, the coefficients of viscous contact damping are determined to provide critical viscous damping that approximates quasi-static loading. The coefficients of viscous contact damping in both normal and shear directions are given by C_n and C_s, respectively, with the following equations:

$$C_n = 2\sqrt{m_{ij}k_n} \tag{6}$$

$$C_s = C_n\sqrt{k_s/k_n} \tag{7}$$

where m_{ij} is given by the mass of two particles m_i and m_j, as follows:

$$m_{ij} = \frac{2m_i m_j}{m_i + m_j} \tag{8}$$

If the stiffness of the springs, k_n, k_s, and k_θ are set as tuning parameters treated independently, a large effort will be required to determine appropriate values for them. Therefore, the stiffness of the normal and rotational springs, k_n and k_θ are calculated using beam theory, and the stiffness of shear springs k_s is calculated by multiplying the stiffness of the normal spring k_n and a constant stiffness ratio α. Thus, the stiffness of the springs given by the following equations:

$$k_n = \frac{E_p A}{L} \tag{9}$$

$$k_s = \alpha k_n \tag{10}$$

$$k_\theta = \frac{E_p I}{L} \tag{11}$$

where A is the cross-sectional area of the bond, and I is the moment of inertia of the bond. E_p is Young's modulus of particle and bonds. The moment of inertia I depends on the shape of the cross-section, and rectangular cross-section is assumed in this study.

Young's modulus E_p assigned to the particles and the stiffness ratio α are microscopic parameters, and these values are different from Young's modulus and Poisson's ratio of the rocks obtained from the laboratory experiments and simulation of the uniaxial compression tests.

The normal stress σ and shear stress τ acting on the cross-section of the bond are calculated using the following equations. The stress and the strain are positive in compression:

$$\sigma = \frac{f_n}{D} \tag{12}$$

$$\tau = \frac{f_s}{D} \tag{13}$$

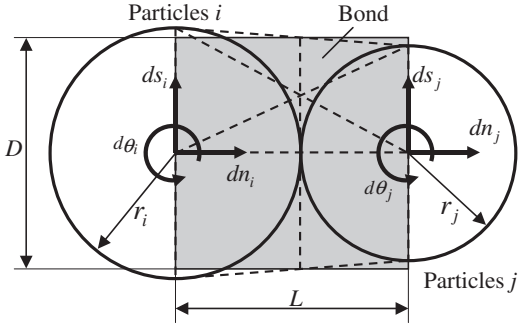

Fig. 1. Bonded particles model.

2.2. Microcrack generation

When σ exceeds the strength of normal spring σ_c or τ exceeds the strength of shear spring τ_c, then the bond breaks and three springs are removed from the model altogether. The criterions for bond break are summarized as follows. They imply that the normal spring breaks only by tension, and compression does not cause the bond breaks.

Bond break criterion 1: $|\sigma| \geq \sigma_c$ and $\sigma < 0$ (tensile stress)
Bond break criterion 2: $|\tau| \geq \tau_c$

Each bond breakage represents the generation of microcracks. A microcrack is generated at the contact point between two particles. A crack length is assumed to be the same as the bond diameter D, and the direction of it is perpendicular to the line joining the two centers.

In the parallel-bond model developed by Potyondy and Cundall [15], the moment acting on the parallel-bond (which is